

# Comparison of Structured Light Projection-based Surface Reconstruction Methods

Imre Forgács<sup>1\*</sup>, Ákos Antal<sup>1</sup>

<sup>1</sup> Department of Mechatronics, Optics and Mechanical Engineering Informatics, Faculty of Mechanical Engineering, Budapest University of Technology and Economics, Műgyetem rkp. 3., H-1111 Budapest, Hungary

\* Corresponding author, e-mail: [forzacsimre@edu.bme.hu](mailto:forzacsimre@edu.bme.hu)

Received: 04 March 2025, Accepted: 28 May 2025, Published online: 04 June 2025

## Abstract

In recent decades, technological advancements and digitalization have led to the emergence of numerous new instruments and measurement techniques in optics. Contactless measurement methods have gained increasing significance, especially since the COVID-19 pandemic. Profilometry, as an optical measurement technique, enables precise and non-destructive surface analysis. Compared to traditional contact-based methods, it offers numerous advantages, making it particularly useful in various fields, especially in medicine. These techniques allow for detailed examination of biological surfaces and tissues without physical contact, which is often crucial for patient safety. They can be applied to analyze skin structure, monitor wound healing, and assess the surface properties of implants and prosthetics while minimizing infection risks and other complications.

Beyond medical applications, profilometric techniques are also widely used in the defense industry, materials science, and manufacturing, where accurate and rapid non-contact surface characterization is essential. Our research explores various types of profilometry and their potential applications using different models. The core principle involves projecting structured light onto a surface and capturing the distorted pattern. The reflected light contains the surface's characteristics, allowing its geometry to be reconstructed through image processing. The most used mathematical tools for this are Fourier and wavelet transforms, the latter often being more efficient due to its scaling and shifting properties. Besides these, other integral transforms can also be applied. In this research, we compare and evaluate different integral transform-based profilometric methods to derive useful conclusions.

## Keywords

fringe projection profilometry, surface reconstruction, Fourier transform, wavelet transform, Hilbert transform

## 1 Introduction

In today's digital world, image processing is one of the most rapidly evolving fields, with applications ranging from medical and biomechanical applications (tissue engineering) to satellite image analysis. The development of optical techniques and image processing methods is gaining more attention each year, alongside the growing demand for contactless measurement methods, particularly in medicine [1]. These techniques are primarily based on mechatronic and optical principles, as exemplified by robotic surgery, with the Da Vinci surgical system being a well-known pioneer [2]. While this solution belongs to the field of telemanipulation, its success highlights the necessity of contact-free methods in healthcare.

One such technique is profilometry, an optical measurement method that enables high-precision, non-destructive 3D surface analysis. A related approach, deflectometry,

is mainly used for inspecting reflective surfaces, detecting topographical deviations with high sensitivity [3]. This method achieves sub-millimeter accuracy over large areas, making it invaluable in quality control and the automotive industry, where it is employed to examine body panel surfaces [4]. However, a significant challenge in deflectometry is the calibration [5].

Both profilometry and deflectometry have multiple variants. Contact profilometry (stylus profilometry) provides highly accurate measurements but is unsuitable for soft or delicate surfaces due to the physical contact involved [6]. Among non-contact methods, Fourier Transform Profilometry (FTP) is widely used, alongside Phase-Measuring Profilometry (PMP), confocal profilometry, and structured pattern detection (SPD) techniques [7]. Advances in computational image processing

have introduced new measurement approaches, including laser profilometry, which relies on triangulation for fast and accurate surface mapping [8].

Fringe projection profilometry, the most relevant technique for this study, projects a known pattern onto a surface and derives geometry from the deformed reflection [9]. It allows fast measurement of large areas, while deflectometry methods like Phase-Measuring Deflectometry (PMD) reconstruct surface normals from distorted phase data [3]. Understanding the limitations of each method is essential for selecting the most suitable approach and ensuring reliable analysis.

## 2 Surface reconstruction methods

This section briefly overviews the most widely used 3D surface reconstruction techniques, highlighting fundamental principles and key challenges. With ongoing developments in surface analysis, both new methods and hybrid approaches are emerging. Optical measurement techniques can be categorized by light source (coherent or non-coherent), surface type (diffuse or reflective), contact nature (contact or non-contact), and resolution scale (microscopic or macroscopic) [10].

### 2.1 Moiré method

The Moiré phenomenon is a commonly observed optical effect encountered in everyday life. A typical example occurs when two layers of finely woven fabric overlap, forming a coarse interference pattern that shifts significantly with minor layer displacement. This effect, illustrated in Fig. 1 [11], originates from the French word "*moiré*", meaning "wavy" or "flame-like" pattern. Physicists have studied the phenomenon since the 19<sup>th</sup> century, and Lord Rayleigh [12] was among the first to propose its use for measurement applications.

The effect arises from the interaction of base gratings, which, in optical terms, are amplitude gratings characterized by their spatial frequency (the number of periods per unit length). When two such gratings overlap, a Moiré pattern forms, which—under a suitable setup—represents the surface contours similarly to topographic

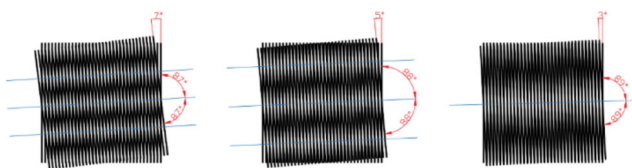


Fig. 1 Moiré fringes of identical gratings with different angular deviations [11]

maps. The Moiré fringes connect points on the examined surface that are equidistant from a reference plane.

This technique can be considered a special case of interference. If one base grating represents the state of an object at time ( $t$ ) and another at a later moment ( $t + 1$ ), the resulting Moiré fringes reveal differences between these states. Consequently, any state of the object can be determined from the other two. More details on this method can be found in [7, 13, 14]. Additionally, it is important to mention that one of the most significant applications of Moiré techniques is in medical imaging, particularly in spinal and posture analysis [11].

There are two main types of the moiré method — shadow moiré and projection moiré — which are well-known and widely studied in optical metrology. Although both techniques are relatively robust and simple to implement, their measurement accuracy strongly depends on the viewing and illumination angles, with typical resolution in the sub-millimeter range. Moiré-based profilometry is commonly used in medical diagnostics (e.g., posture or spinal analysis), material deformation studies, and mechanical strain visualization [11–14].

Overall, the moiré method is a well-established and effective technique with a wide range of applications.

### 2.2 Binary and gray code

Binary and gray code methods belong to the category of sequential 3D surface reconstruction techniques [15]. These approaches determine the three-dimensional shape of a surface by encoding and decoding projected patterns. They use black and white stripes to represent the projected pattern, ensuring that each point on the object's surface is assigned a unique binary code for differentiation.

In general, an  $N$  pattern sequence can encode  $2^N$  stripes, requiring multiple images for accurate measurement. The key advantages of this method are its simplicity, robustness, and reliability due to the binary encoding. However, resolution is limited by computational capacity, as achieving higher resolution necessitates projecting more stripes onto the surface.

These techniques are widely used in robotics, cultural heritage 3D documentation, and machine vision. Further details on phase-shifting, gray code methods, and their combinations can be found in [15].

### 2.3 Stripe indexing

Stripe indexing is a single-shot technique for 3D surface reconstruction that determines surface topography from a

single image. This makes it particularly advantageous for capturing moving objects or dynamic scenes where multi-frame methods, such as phase-shifting, are unreliable. Since only one image is required, these techniques enable fast surface reconstruction.

However, single-image measurements generally have lower resolution and accuracy than multi-frame approaches due to limited available information [16]. Additionally, decoding complex patterns can be challenging in noisy environments or on surfaces with uniform color and texture. Despite these limitations, stripe indexing is widely used in medical applications for rapid face and body scanning, as well as in industrial quality control, where speed is critical.

The general workflow of stripe indexing consists of:

1. Pattern projection: The object's geometry distorts the pattern.
2. Image capture: A camera records a single image of the surface with the deformed pattern.
3. Pattern decoding: Different decoding algorithms are used depending on the pattern type.
4. Reconstruction: This can be done using relative or absolute coordinates, employing geometric or conventional calibration methods [17], ultimately generating the 3D model.

This technique has several variations, as stripe indexing can follow different rules. For instance, a color camera can be used with colored stripes. One advantage of this approach is that it assigns indices based on colors, eliminating errors that may arise with black-and-white or gray-scale coding. Additionally, it enables real-time imaging and is among the most precise methods.

Stripe indexing techniques are generally robust and fast, but their accuracy is limited by pattern complexity and highly sensitive to surface texture and illumination conditions. These methods are widely used in face and body scanning, medical imaging, and rapid industrial quality control where speed is critical.

### 2.4 Grid indexing

Grid indexing is a fast, single-image 3D reconstruction method using uniquely identifiable grid patterns to map surface points. Like stripe indexing, it offers speed and motion tolerance but can be sensitive to noise and surface color due to its reliance on color-coded grids. Its applications are similar to those of other pattern-based techniques.

Different grid indexing strategies exist depending on the encoding approach [16]. One common method uses color-coded vertical and horizontal grid lines to create unique indices. Another widely used strategy employs a pseudo-random binary array (PRBA) to generate grid locations, marking them with points or patterns so that any window or sub-window maintains a unique encoded pattern. Alternatively, a multi-valued pseudo-random array can replace PRBA, using specialized codewords instead of points to form a distinctive projection pattern, as illustrated in Fig. 2.

A final approach involves two-dimensional color-coded dot arrays. Though effective, this method requires a more time-consuming algorithm. Further details on this approach and its corresponding algorithm can be found in [18].

There are numerous approaches to enhancing the performance of 3D surface analysis systems by combining multiple encoding schemes mentioned above to improve specific aspects. These newly developed techniques fall under the category of hybrid methods.

Phase-shifting is one of the most widely used sequential methods in 3D surface reconstruction, based on projecting a sinusoidal pattern and capturing multiple phase-shifted images to compute the surface geometry. It provides high accuracy and efficient data processing but is sensitive to motion and external disturbances due to its multi-frame nature. Its typical applications include skin and tissue analysis in medical imaging and defect detection in precision components. The method is highly precise (often at micrometer level), but its performance depends on accurate phase unwrapping and careful calibration, making it sensitive to both environmental conditions and parameter settings.

### 2.5 Phase shifting

Among sequential methods, the most widely used is phase-shifting, which relies on a series of structured patterns for measurement. The principle involves projecting a

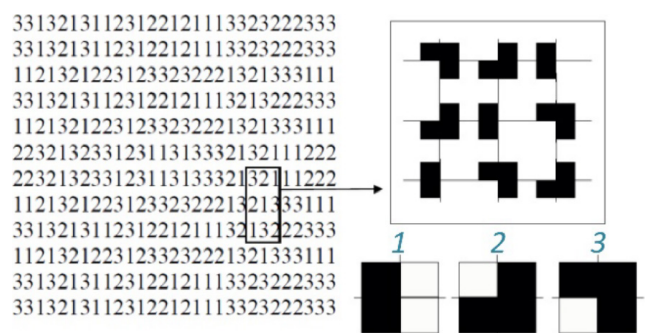


Fig. 2 Use of mini-patterns as codewords for grid indexing [16]

periodic light pattern, typically a sinusoidal grid, onto the target surface and shifting its phase in multiple steps [16]. By capturing several images at different phase shifts, the surface topography can be computed.

This method offers high accuracy and efficient data processing but is highly sensitive to motion and external conditions. Since multiple images must be acquired sequentially, even minimal movement of the pattern, measurement system, or object can introduce errors [19]. Phase-shifting techniques are widely applied in medical imaging for analyzing skin and tissue surfaces, as well as in industry for detecting surface defects in precision components.

The measurement process follows these steps:

1. Structured light projection: A sinusoidal grid pattern with known frequency and phase is projected onto the surface.
2. Phase shifting: The pattern's phase is shifted in discrete steps, typically  $0^\circ$ ,  $90^\circ$ ,  $180^\circ$ , and  $270^\circ$ , with an image captured at each shift.
3. Image acquisition: The camera records the distorted pattern at each phase shift, encoding the surface's geometric information.
4. Phase calculation.
5. Phase unwrapping: The calculated phase values range from 0 to  $2\pi$ . A phase unwrapping algorithm reconstructs a continuous phase profile.
6. Height calculation.

### 2.6 Deflectometry

Phase Measuring Deflectometry (PMD) is a non-contact method used to analyze smooth, reflective surfaces in 3D with micrometer-level accuracy [3]. It uses a camera and projection system to capture reflected sinusoidal patterns, from which surface normals and curvatures are computed.

PMD stands out due to its high accuracy, large dynamic range, and ability to measure entire surfaces simultaneously. As a non-contact method, it is particularly suitable for analyzing sensitive, reflective surfaces such as mirrors, lenses, optical components, and polished metals. More details on deflectometry and its variations can be found in [20–22].

Profilometry and deflectometry are closely related surface analysis techniques, particularly Phase Measuring Profilometry (PMP) and PMD. Their differences are illustrated in Fig. 3. In profilometry, a projection system with imaging optics casts a structured pattern (e.g., parallel fringes) onto a surface. The deformations of this pattern, captured from a different angle, reveal the surface shape. In contrast, PMD does not use imaging optics. Instead, a pattern is displayed on a screen (e.g., a monitor), and the test surface acts as an imaging element (e.g., a mirror), forming a reflected image that is recorded and analyzed.

Despite differences in optical setup (Fig. 3), PMD and PMP share similar data processing challenges, including phase retrieval and nonlinearity in digital light projection systems [21]. While both techniques derive 3D shape information from the geometric relationship between the source and detectors, their mathematical and physical principles differ. PMP relies on optical triangulation to measure diffuse surfaces, whereas PMD analyzes reflective surfaces based on the law of reflection. Additionally, PMP phase values directly correspond to height data, whereas in PMD, phase values encode both slope and height information.

### 3 Profilometry

Profilometry is a powerful surface analysis technique that enables precise three-dimensional characterization of objects. It can be categorized into two main types based on contact with the measured object: contact and non-contact

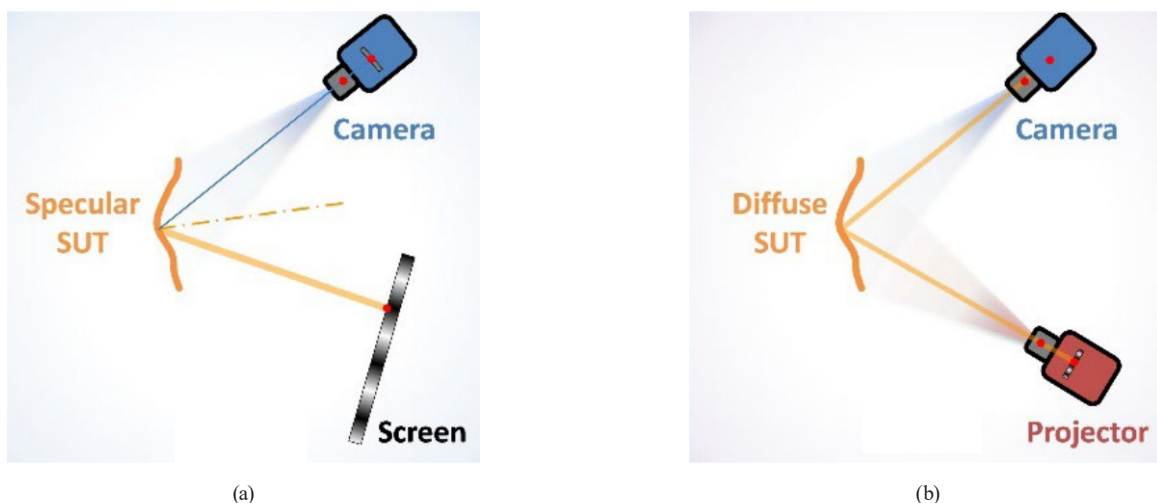


Fig. 3 The general measurement setup of (a) Phase Measuring Deflectometry and (b) Phase Measuring Profilometry [3]

(optical) profilometry, such as confocal microscopy and interferometry. Non-contact profilometry offers clear advantages, including its versatility and the elimination of physical interaction, making it particularly valuable in medical applications [9]. By avoiding direct contact, it helps prevent hospital-acquired infections and facilitates low-risk examination of the back, neck, and spine (e.g., scoliosis), as well as delicate structures like blood vessels and internal organs [23, 24].

Structured light projection is widely utilized due to its extensive measurement range and high resolution, accommodating objects from a few micrometers to several meters in size. This makes it a crucial tool in both scientific research and industrial applications, including:

- Dentistry and medical diagnostics [25, 26],
- Vibration analysis [27],
- Skin and wound monitoring [28],
- Corrosion analysis [29],
- Surface roughness measurement [30].

Beyond these applications, profilometry is employed in hearing aid design and the automotive industry. For instance, it enables the analysis of airbag deployment, providing critical data for design optimization and safety testing. Another intriguing case extends beyond forensic and law enforcement applications to modern digital technologies. The structured light technique's ability to deliver high-resolution, full-field 3D reconstruction in a non-contact manner [9] makes it ideal for applications in video games and virtual reality.

Despite its widespread adoption and success in industry and research, profilometry has inherent limitations, such as dependency on surface properties and environmental conditions, leading to geometric constraints. However, when these factors are considered during method selection and application, highly accurate results can be achieved. As a contactless measurement technique, profilometry benefits from a straightforward experimental setup (Fig. 4). A complete measurement can be performed using standard laboratory equipment, including a data-processing computer, a projector, and an imaging device - camera. Fig. 4 illustrates the general setup and imaging process of a profilometric measurement.

Once the measurement setup is complete and all necessary components are in place, as shown in Fig. 4, the measurement process can begin. The overall structure remains similar across different methods.

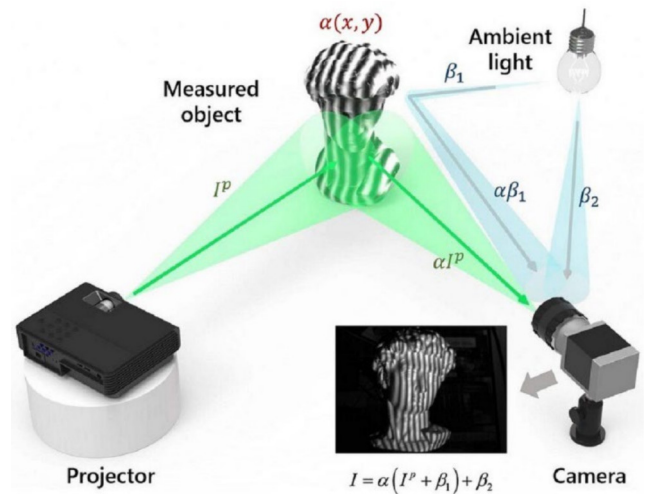


Fig. 4 The imaging process and setup of fringe projection profilometry (FPP): pattern projection, reflection, and image acquisition [19]

The initial step (if required) is the optical calibration of the camera and projector to determine their intrinsic and extrinsic parameters. However, this step can be omitted when using modern cameras and projectors, as relative coordinates in shape reconstruction can yield meaningful results without explicit calibration.

The first essential step is structured pattern projection onto the target object, followed by capturing the reflected, distorted pattern. The subsequent phases involve image or data processing, which can be further divided depending on the applied method or mathematical approach. Generally, profilometric surface reconstruction consists of two main stages: image acquisition and data processing.

The second stage can be further divided into three key steps. Once projection and data collection are complete, the next crucial step is fringe pattern analysis and phase computation. A fundamental part of this process is phase unwrapping [31], which resolves phase ambiguities caused by the periodic nature of inverse trigonometric functions, defined only in the  $[-\pi, \pi]$  range. Proper unwrapping techniques are essential to prevent errors.

The final step in profilometric image processing is system calibration, which reconstructs 3D shapes by linking real-world and image coordinates [17]. This can be done using relative positioning of system components or by applying standard optical calibration methods to determine intrinsic and extrinsic parameters.

#### 4 Mathematical tools of profilometry

Profilometric techniques can be categorized in various ways, but the most common classification is based on the

analysis and evaluation of fringe patterns. This categorization primarily depends on the mathematical domain in which data processing occurs. Fringe pattern analysis can be performed using several mathematical transformations, including Fourier, wavelet, Gabor, Hilbert, and S-transforms [32, 33]. Additionally, many other methods exist, with numerous variations of each transformation [34]. Our research explores and models three profilometry variants that require only a single image for execution. The study in [19] provides a comparative analysis of various phase-shifting methods, like our approach. Several mathematical techniques are available for analyzing reflected and deformed patterns, and they can be classified based on different criteria. For instance, profilometric methods can be divided into spatial or temporal techniques, depending on whether a single or multiple images are required for data processing. Additionally, they can be categorized based on whether image processing is performed in the frequency domain or not.

#### 4.1 Fourier transformation profilometry

Fourier Transformation Profilometry (FTP) [23] emerged after phase-shifting interferometry and gained widespread adoption before the turn of the millennium [32–35]. Its development was driven by the increasing use of Fourier transformation in image and signal processing, as well as advancements in modern cameras and computing power, which enabled faster data processing and the efficient implementation of complex procedures. Early FTP was often referred to as the Takeda method, as Takeda was the first to publish on the subject [36].

Initially, the method utilized one-dimensional transformations, later expanding to two-dimensional applications. Despite this evolution, FTP offers significant advantages, such as requiring only a single image for measurement—unlike phase-shifting methods—allowing dynamic objects to be analyzed. This also accelerates the contactless measurement process. However, FTP is highly sensitive to optical aberrations and environmental noise, making phase unwrapping a challenging task. The operating principle of FTP aligns with general surface reconstruction techniques, with the key distinction that a Fourier transform is applied to the captured image. This transformation shifts the image data into the frequency domain, enabling the separation and analysis of different frequency components.

#### 4.2 Wavelet transform

In addition to the previously discussed Fourier Transform (FT), alternative methods such as the Hilbert Transform,

and the Wavelet Transform (WT) can also be applied [33]. Although the Hilbert Transform was introduced in the early 20<sup>th</sup> century, it was primarily used in mathematics and only later adopted in image processing. In contrast, the WT emerged as a novel approach in the 1990s and has since been extensively researched and applied [37, 38]. Various types of wavelet transforms exist, including early versions based on simple functions, such as the step function and the Morlet wavelet. In signal and image processing, biorthogonal wavelet families are widely used due to their linear phase properties. In profilometry, complex mother wavelets are particularly effective for analyzing fringe patterns, with notable families including Paul, Shannon, and Complex Gaussian wavelets. Additionally, Meyer and Gaussian wavelets belong to the class of real-valued wavelets. Further details on wavelet families and their theoretical background can be found in [37], while practical implementations are available in MATLAB's Wavelet Toolbox documentation [39].

Both the FT and WT offer different approaches to analyzing signals and images [34]. The FT decomposes a signal into sinusoidal components, providing frequency information with precise amplitude and phase values. However, it lacks localization, meaning it does not indicate when or where specific frequencies appear within the signal. This limitation makes it unsuitable for analyzing signals with time-varying frequency content, as signals with identical frequencies but different time intervals yield the same Fourier representation [33]. Consequently, FT is mainly used for analyzing stationary signals and frequency-domain characteristics, such as in spectrum analysis.

WT, on the other hand, enables simultaneous time-frequency (or space-frequency) analysis by decomposing signals into localized wavelets—finite-duration functions with zero mean. This decomposition allows for precise frequency localization while preserving temporal or spatial information. Unlike FT, WT does not rely on sinusoidal functions but instead scales and shifts the mother wavelet to extract localized features [40, 41]. This approach reduces artifacts from overlapping components, leading to more accurate edge analysis in images. Moreover, WT computations require only the signal values and their negations, eliminating the need for trigonometric functions.

Despite its advantages, WT involves more complex computations than FT, as it provides additional information on the signal's time or spatial distribution. The fundamental difference between the two methods lies in the analysis function: FT uses infinite, symmetric sinusoidal waves of varying frequencies, whereas WT employs irregular,

asymmetric, and finite-duration wavelets (Fig. 5). This distinction significantly impacts the type of information obtained. Furthermore, both continuous and discrete wavelet transforms (CWT and DWT) are widely used [37]. In digital signal and image processing, DWT is more prevalent due to its discrete nature. The primary difference is that CWT operates across all scales with continuous shifts of the wavelet, making it useful for various applications. Overall, WT is better suited for analyzing non-stationary signals with varying frequency components.

### 4.3 Hilbert Transform

The Hilbert Transform (HT) is a widely used mathematical tool in image and signal processing [42–44]. Various methods exist for extracting 3D shape information from distorted reflection patterns, with phase-shifting techniques, Fourier transform (FT), wavelet transform (WT), and Hilbert transform being among the most significant. These three transforms are often compared or used interchangeably due to their similar applications but distinct characteristics. A detailed comparison of FT, WT, and Hilbert-Huang Transform (HHT) is provided in [45].

HHT, a modern extension of the classical HT, was developed by Huang around 1998, nearly a century after the original mathematical concept was introduced by David Hilbert in the early 20<sup>th</sup> century. While FT requires transforming signals into the frequency domain, HT operates within the same domain, simplifying computations. This property reduces computational complexity, though HT remains one of the more intricate methods.

HT is a linear operator and can cause phase reversal of the original signal [42]. Its key mathematical properties include:

1. The HT of a real function is linear.
2. Applying HT twice results in the negative of the original function.
3. The HT of a function's derivative is equivalent to the derivative of its HT.
4. A function and its HT are orthogonal.

HT shifts the input signal's phase by 90°, meaning a sine wave input results in a cosine wave output. Its linearity makes it effective for analyzing frequency components but limits its ability to process nonlinear signals. HHT addresses this by enabling the analysis of non-stationary and nonlinear signals. Both HT and HHT are widely used in digital filter design, radar systems, medical imaging, and other image processing applications [43]. Further details on HT and Hilbert-based profilometry can be found in [44–46].

Overall, these transformation methods are crucial tools in both industry and research. Each has unique advantages and limitations, making the choice of technique dependent on the specific application and conditions.

### 5 Application and results

In this section, we present the application of wavelet, Fourier, and Hilbert transform-based profilometry, along with our results on generated surfaces. For inquiries regarding the program codes, models, and solution methods used in this research, feel free to contact us via email or in person. While we have not prepared separate documentation for these algorithms, we have included detailed comments to highlight key sections. The MATLAB codes were developed based on the previously discussed

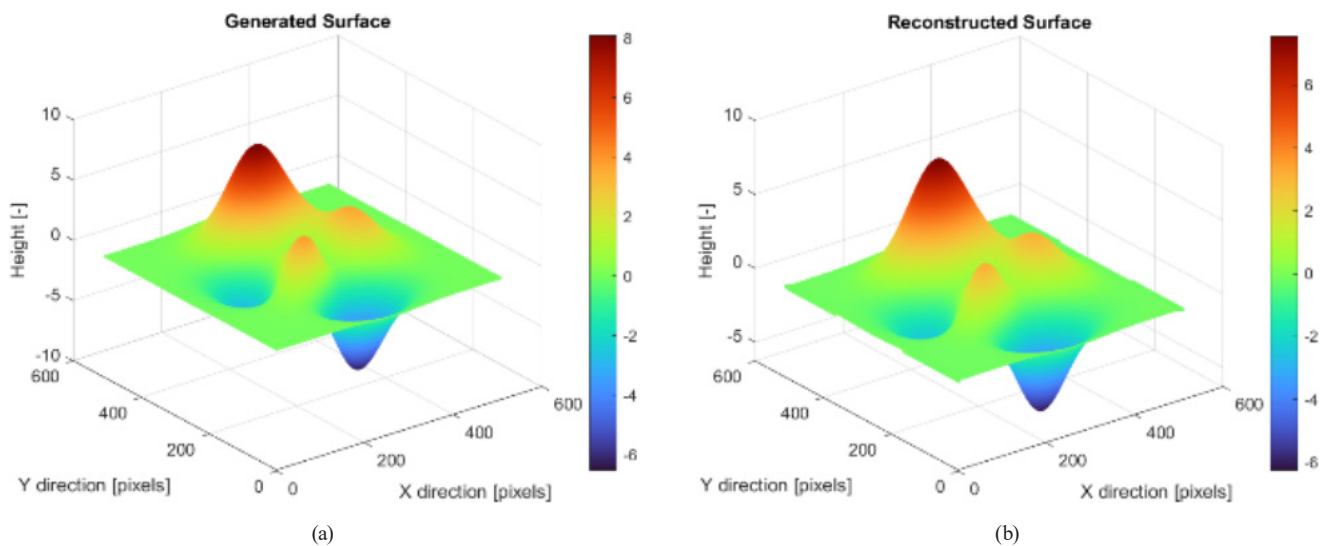


Fig. 5 (a) The original generated surface and (b) the reconstructed surface with Wavelet transform

techniques and literature, using the MATLAB R2023a computing platform [39].

### 5.1 Wavelet transform-based profilometry

All implementations are demonstrated on a sufficiently complex surface generated using the MATLAB *peaks()* function [39]. This method produces a surface formed by a scaled and transformed combination of multiple Gaussian functions, depending on the chosen parameters. As a result, the surface features smoother transitions than a cube while being more complex and visually informative than a flat plane or a simple curve, making it an ideal choice for model testing.

The first step in testing is generating the surface and the striped pattern. Next, the pattern is distorted by the surface in a controlled environment. The final step involves processing the data and reconstructing the surface using the wavelet transform-based method, as described earlier.

Fig. 5 illustrates the results: Fig. 5 (a) shows the original artificially generated surface, while Fig. 5 (b) presents the reconstructed shape obtained through wavelet transform profilometry.

Fig. 5 illustrates that the original surface was successfully reconstructed almost flawlessly using the wavelet transformation method. However, slight discrepancies at the edges of the restored surface are observed compared to the original. Therefore, we also calculated the difference between the two surfaces and created a so-called error surface by subtracting the original shape from the restored one. The error of the applied technique is shown in Fig. 6.

The difference between the reconstructed and the original surface is negligible and mainly occurs at the edges,

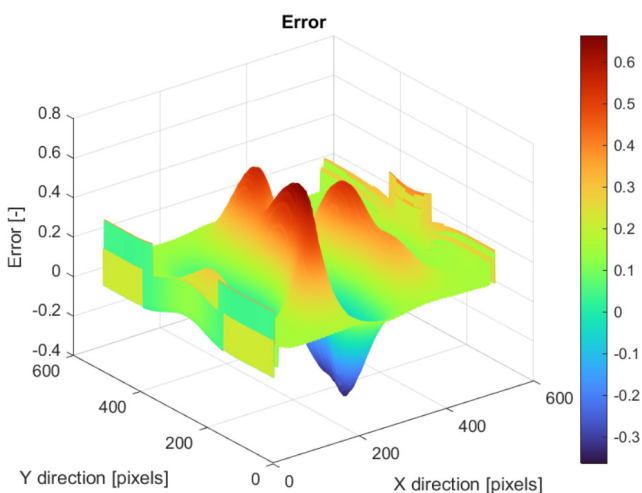


Fig. 6 The difference between the original and the restored surfaces in case of wavelet transform-based profilometry

as shown in Fig. 5 and Fig. 6. Of course, a similar situation arises when examining different shapes, for example, those with more abrupt or less contrasting small changes on their surface.

Overall, with wavelet transformation profilometry, we successfully reconstructed the generated surfaces throughout all tests. Despite the minor deviations, the measurements performed on the presented artificially generated surfaces clearly demonstrate the properties and effectiveness of the applied wavelet transformation method.

### 5.2 Fourier transform-based profilometry

The Fourier transform-based profilometry was implemented and tested similarly to the wavelet and Hilbert transform methods. Since the MATLAB implementation [39] was built upon the previously introduced approach, only minor modifications were required to adapt the algorithm to Fourier transform principles while ensuring its efficiency.

It is important to note that all three algorithms were tested on multiple surfaces with varying characteristics, yielding comparable accuracy to the results presented here. The pattern and surface generation, as well as the distortion process, followed the same methodology as in the wavelet transform (WT) approach. Consequently, the distorted pattern evolved similarly, and the generated surface remained unchanged, as no modifications were made to the generation procedure. The fundamental difference was the replacement of the wavelet transform with the Fourier transform and the necessary adjustments to align the algorithm with its properties. Fig. 7 illustrates the results: the left side (Fig. 7 (a)) shows the original generated surface, while the right side (Fig. 7 (b)) presents the reconstructed shape obtained through Fourier transform profilometry.

Fig. 7 demonstrates that the original generated surface was reconstructed with near-perfect accuracy using the Fourier transform method, achieving even greater precision than the wavelet transform approach. In this case, discrepancies between the initial and reconstructed geometries are barely noticeable, though the WT method also exhibited only minimal deviations. For a more comprehensive comparison, we calculated the difference between the original and reconstructed surfaces, with the spatial representation shown in Fig. 8.

The error associated with the surface shown in Fig. 7 (see Fig. 8) is on the order of for the Fourier transform method, significantly lower than the corresponding value for the WT

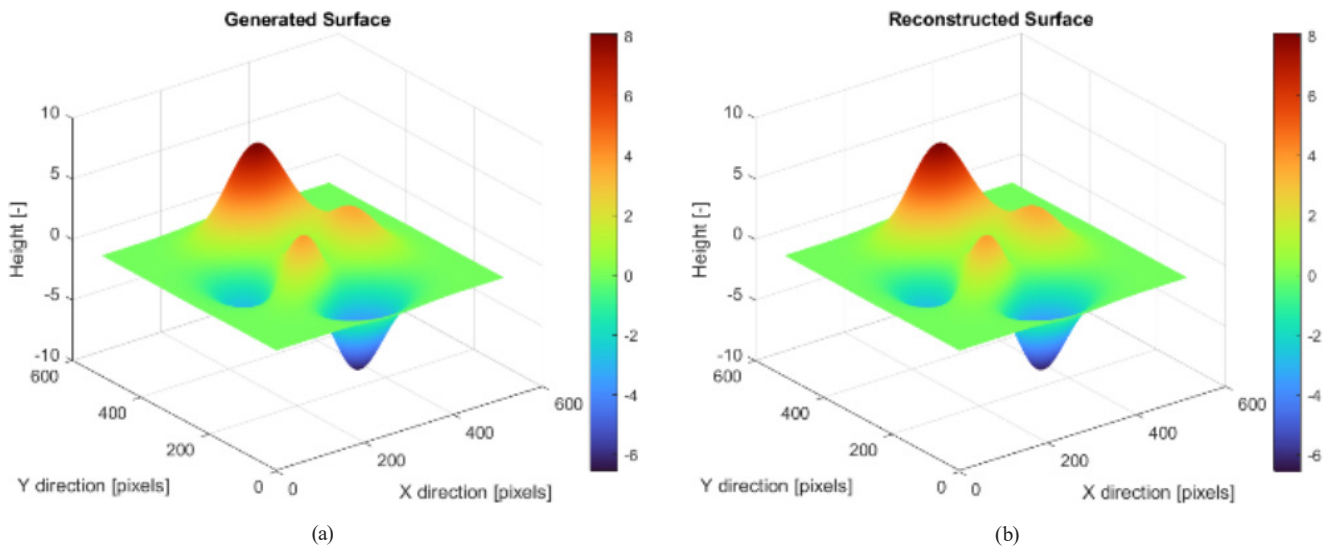


Fig. 7 (a) The original surface and (b) the reconstructed surface with Fourier transform

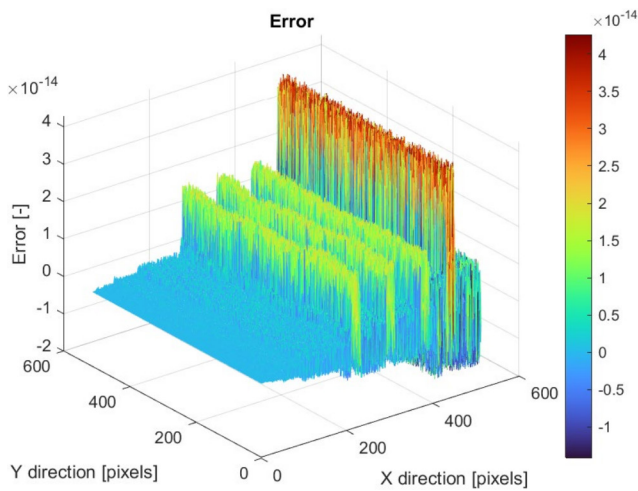


Fig. 8 The difference between the original and the restored surfaces in case of Fourier-transform-based profilometry

approach (Fig. 6). Similar accuracy was achieved for other artificially generated geometries, with negligible error. Overall, Fourier transform profilometry demonstrates high accuracy in reconstructing synthetic surfaces.

### 5.3 Hilbert transform-based profilometry

To ensure clarity and effective comparison, we followed the same principles as in previous approaches. The surface generation and distortion steps remained unchanged, with modifications applied only to the second phase of the algorithm. Specifically, the transformation method was replaced, and key parameters were adjusted according to relevant literature to fit our measurements. After these modifications, the final reconstructed surface was obtained using the unwrapped phase map, following the previously described methodology. Fig. 9 presents the

original surface alongside the geometry reconstructed via the Hilbert transform.

In this case, the initial generated surface was successfully reconstructed. However, a minor deviation can be observed on the left side (closer edge) of the reconstructed geometry, which does not appear elsewhere. Across the rest of the surface, the error remains negligible. This phenomenon is clearly visible in Fig. 10, which presents the error surface associated with the Hilbert transform.

### 5.4 Comparison and evaluation

In all presented MATLAB implementations [39], we highlight results where the characteristic properties and differences of each transformation are most apparent. Consequently, broad conclusions cannot always be drawn regarding profilometry processes using different transformations. As in our code, several steps and parameters are adjustable, leading to varying outputs from identical inputs. However, the comparison remains relevant to our specific MATLAB implementations [39] and the fundamental structure of the algorithms.

Notably, the smallest discrepancy between the original and reconstructed surfaces occurs with the Fourier transform. In contrast, wavelet (WT) and Hilbert (HT) transforms yield errors of similar magnitude but different distributions. The WT-induced deviation closely follows the surface topography: minimal in flat areas and more pronounced in regions with abrupt changes. As a result, WT errors distribute more evenly across the shape, making them less visually prominent in reconstructions. Conversely, the HT-associated error is more noticeable since it does not follow the surface geometry uniformly. Instead, it tends to

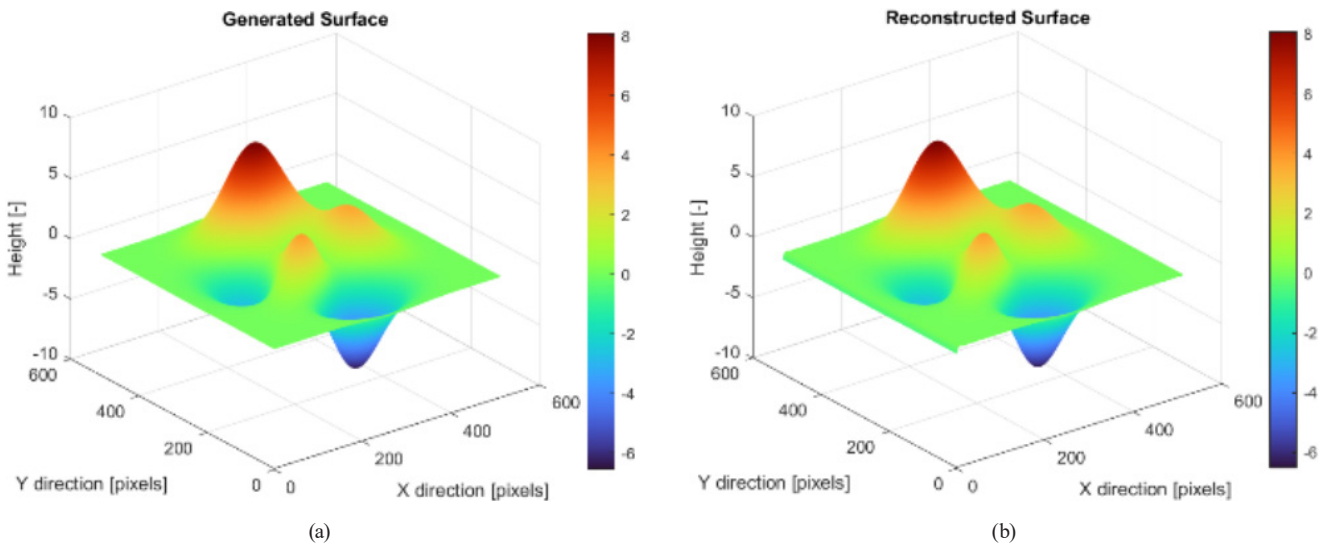


Fig. 9 (a) The original surface and (b) the reconstructed surface with Hilbert transform

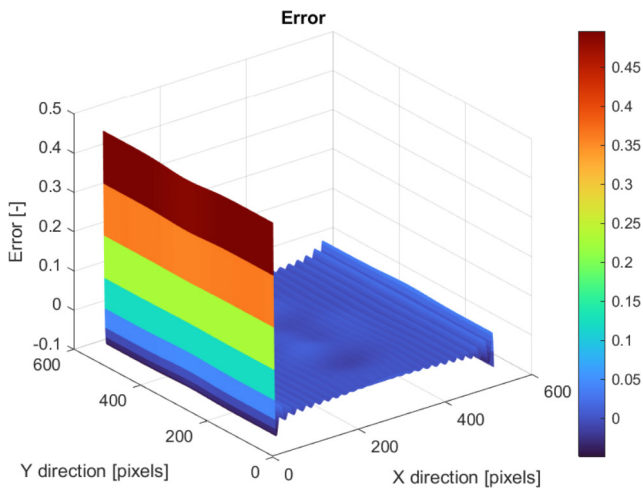


Fig. 10 The difference between the original and the restored surfaces in case of Hilbert transform-based profilometry

accumulate at the edges—typically more on one side—while the central region exhibits negligible deviation, similar to the Fourier transform. This behavior is also influenced by the boundary effects of the applied transforms, which become more pronounced when local features or sudden transitions occur near the edges of the surface.

Each transform-based profilometry method offers distinct advantages and limitations, depending on the nature of the surface being analyzed and the specific requirements of the application. Fourier Transform Profilometry (FTP) is straightforward to implement, computationally efficient, and highly accurate when dealing with smooth, periodic, or globally structured surfaces. Its major limitation, however, lies in its global nature: it lacks spatial localization, making it less effective when analyzing surfaces with localized or non-stationary features. Additionally, its

sensitivity to high-frequency noise and phase discontinuities can lead to reconstruction errors, particularly in areas with sharp edges or complex geometries.

Hilbert Transform (HT)-based profilometry represents a lightweight alternative with relatively simple computation, as it avoids full frequency-domain processing. While HT can provide accurate phase information in many cases, its reconstructions often suffer from directional bias, especially near the image boundaries. The method does not adapt well to localized surface features, and the errors it introduces often manifest asymmetrically, typically along one axis. This makes it less robust in applications requiring high geometric fidelity across the entire surface.

In contrast, Wavelet Transform (WT)-based profilometry offers the greatest adaptability among the evaluated methods. Unlike the global nature of FT and the directional sensitivity of HT, WT enables multi-resolution analysis, allowing both local and global features to be captured effectively. The method benefits from a wide selection of mother wavelets and tunable parameters, such as scale and translation, which make it highly customizable for various types of surfaces and noise conditions. These properties also explain why WT errors are generally more uniformly distributed and conform more closely to the surface profile. While WT requires more careful tuning and is computationally more demanding, its scalability, shift invariance, and parameter flexibility make it especially suitable for real-world applications, where surface complexity and measurement conditions vary. In practice, the ability to choose an appropriate wavelet basis and adapt its parameters to a specific measurement task is a significant advantage—something that is not available to the same extent in FT or HT methods.

Finally, it is worth noting that all transform-based profilometry techniques are affected by the properties of the reconstructed surface itself. The spatial frequency content, curvature, and abrupt transitions directly influence the reconstruction error, and different methods respond differently to these challenges. While FT and HT are more prone to producing artifacts in the presence of sharp discontinuities, WT can better adapt to such irregularities, assuming proper parameterization is used. This reinforces our conclusion that method selection should be task-specific, and in many complex or practical scenarios, WT is likely the most robust and versatile choice.

## 6 Summary

Profilometry enables the contactless, non-destructive examination of an object's three-dimensional structure. This technique plays a crucial role in various industries, including automotive manufacturing, production technology, and medical applications.

## References

- [1] Nagy, Á. "Koraszülött csecsemők légzésének és aktív, valamint alvó fázisainak érintésmentes, kamera alapú monitorozása" (Non-contact, Camera-based Monitoring of Respiration and Active and Sleep Phases in Preterm Infants), PhD Thesis, Pázmány Péter Katolikus Egyetem, 2023. (in Hungarian)  
<https://doi.org/10.15774/PPKE.ITK.2023.009>
- [2] Freschi, C., Ferrari, V., Melfi, F., Ferrari, M., Mosca, F., Cuschieri, A. "Technical review of the da Vinci surgical telemanipulator", *The International Journal of Medical Robotics and Computer Assisted Surgery*, 9(4), pp. 396–406, 2013.  
<https://doi.org/10.1002/rcs.1468>
- [3] Huang, L., Idir, M., Zuo, C., Asundi, A. "Review of phase measuring deflectometry", *Optics and Lasers in Engineering*, 107, pp. 247–257, 2018.  
<https://doi.org/10.1016/j.optlaseng.2018.03.026>
- [4] Faber, C., Olesch, E., Krobot, R., Häusler, G. "Deflectometry challenges interferometry: the competition gets tougher!", In: *Proceedings of SPIE: Interferometry XVI: Techniques and Analysis*, San Diego, CA, USA, 2012, 84930R. ISBN 9780819492104  
<https://doi.org/10.1117/12.957465>
- [5] Deng, X., Gao, N., Zhang, Z. "A calibration method for system parameters in direct phase measuring deflectometry", *Applied Sciences*, 9(7), 1444, 2019.  
<https://doi.org/10.3390/app9071444>
- [6] Teague, E. C., Scire, F. E., Baker, S. M., Jensen, S. W. "Three-dimensional stylus profilometry", *Wear*, 83(1), pp. 1–12, 1982.  
[https://doi.org/10.1016/0043-1648\(82\)90335-0](https://doi.org/10.1016/0043-1648(82)90335-0)
- [7] Nochta, G., Antal, Á. "Ortopédiai célú deflektometriai képek Fourier-módszeres feldolgozása" (Fourier-based Processing of Deflectometric Images for Orthopedic Applications), *Biomechanica Hungarica*, 9(1), pp. 41–49, 2017. (in Hungarian)  
<https://doi.org/10.17489/biohun/2016/1/01>
- [8] Kaller, O., Boleček, L., Kratochvíl, T. "Profilometry scanning for correction of 3D images depth map estimation", In: *Proceedings ELMAR-2011, Zadar, Croatia, 2011*, pp. 119–122. ISBN 978-1-61284-949-2 [online] Available at: <https://ieeexplore.ieee.org/abstract/document/6044315> [Accessed: 28 February 2025]
- [9] Gorthi, S. S., Rastogi, P. "Fringe projection techniques: Whither we are?", *Optics and Lasers in Engineering*, 48(2), pp. 133–140, 2010.  
<https://doi.org/10.1016/j.optlaseng.2009.09.001>
- [10] Hu, Y., Chen, Q., Feng, S., Zuo, C. "Microscopic fringe projection profilometry: A review", *Optics and Lasers in Engineering*, 135, 106192, 2020.  
<https://doi.org/10.1016/j.optlaseng.2020.106192>
- [11] Bogdán, C. "The Moiré Method and its Application in Scoliosis", [pdf] In: *Proceedings of the 4<sup>th</sup> International Interdisciplinary 3D Conference, Pécs, Hungary, 2018*, pp. 81–87. ISBN 978-963-429-267-8 Available at: [https://eprints.sztaki.hu/9623/1/Proceedings\\_4th-3D-Conf-2018\\_30385910\\_ny.pdf](https://eprints.sztaki.hu/9623/1/Proceedings_4th-3D-Conf-2018_30385910_ny.pdf) [Accessed: 28 February 2025]
- [12] MOMÉ "A moiré-jelenségről" (The Moiré Effect), [online] Available at: <https://visualgrammar.mome.hu/2016/08/02/manualitas/> [Accessed: 28 February 2025] (in Hungarian)
- [13] Antal, Á. "Optikai úton generált Moiréfelületek hibaanalízise és identifikálása mérés technikai alkalmazásokkal" (Error Analysis and Identification of Optically Generated Moiré Patterns for Metrological Applications), PhD Dissertation, Budapest University of Technology and Economics, 2015. [online] Available at: <https://www.proquest.com/openview/78e12b9b8543edabe58405dea3ce9965/1?pq-origsite=gscholar&cbl=2026366&diss=y> [Accessed: 28 February 2025] (in Hungarian)
- [14] Stricker, J. "Analysis of 3-D phase objects by moiré deflectometry", *Applied Optics*, 23(20), pp. 3657–3659, 1984.  
<https://doi.org/10.1364/AO.23.003657>

Based on our research and the artificially generated test surfaces, all three transformation-based methods successfully achieved high accuracy in reconstructing the generated shapes. The Fourier transform (FT) provided the most precise results; however, it is less robust and adaptable to different measurement tasks compared to the wavelet transform (WT). Notably, the Hilbert transform (HT) yielded accuracy comparable to FT, except for errors concentrated at surface edges. Consequently, while the Fourier Transform achieved the lowest absolute error, the Hilbert Transform also produced highly accurate reconstructions, particularly in central regions, making it a viable alternative in specific cases. Among the three approaches, WT offers the highest degree of flexibility and optimization potential due to its tunable parameters. Consequently, it stands out as the most robust method, best suited for real-world applications based on our findings.

- [15] Zhang, Y., Yilmaz, A. "Structured light based 3D scanning for specular surface by the combination of gray code and phase shifting", *The International Archives of the Photogrammetry, Remote Sensing and Spatial Information Sciences*, XLI-B3, pp. 137–142, 2016.  
<https://doi.org/10.5194/isprs-archives-XLI-B3-137-2016>
- [16] Geng, J. "Structured-light 3D surface imaging: a tutorial", *Advances in Optics and Photonics*, 3(2), pp. 128–160, 2011.  
<https://doi.org/10.1364/AOP.3.000128>
- [17] Talebi, R., Johnson, J., Abdel-Dayem, A. "Binary code pattern unwrapping technique in fringe projection method", [pdf] In: *Proceedings of the 2013 International Conference on Image Processing, Computer Vision, and Pattern Recognition (ICCV'13)*, Las Vegas, NV, USA, 2013, pp. 499–505. ISBN 1-60132-254-2 Available at: [http://worldcomp-proceedings.com/proc/proc2013/ipcv/ICPV\\_Papers.pdf](http://worldcomp-proceedings.com/proc/proc2013/ipcv/ICPV_Papers.pdf) [Accessed: 28 February 2025]
- [18] Griffin, P. M., Narasimhan, L. S., Yee, S. R. "Generation of uniquely encoded light patterns for range data acquisition", *Pattern Recognition*, 25(6), pp. 609–616, 1992.  
[https://doi.org/10.1016/0031-3203\(92\)90078-W](https://doi.org/10.1016/0031-3203(92)90078-W)
- [19] Zuo, C., Feng, S., Huang, L., Tao, T., Yin, W., Chen, Q. "Phase shifting algorithms for fringe projection profilometry: A review", *Optics and Lasers in Engineering*, 109, pp. 23–59, 2018.  
<https://doi.org/10.1016/j.optlaseng.2018.04.019>
- [20] Tang, Y., Su, X., Wu, F., Liu, Y. "A novel phase measuring deflectometry for aspheric mirror test", *Optics Express*, 17(22), pp. 19778–19784, 2009.  
<https://doi.org/10.1364/OE.17.019778>
- [21] Guo, H., He, H., Chen, M. "Gamma correction for digital fringe projection profilometry", *Applied Optics*, 43(14), pp. 2906–2914, 2004.  
<https://doi.org/10.1364/AO.43.002906>
- [22] Xu, Y., Gao, F., Jiang, X. "A brief review of the technological advancements of phase measuring deflectometry", *Photonix*, 1(1), 14, 2020.  
<https://doi.org/10.1186/s43074-020-00015-9>
- [23] Hanafi, A., Gharbi, T., Cornu, J.-Y. "In vivo measurement of lower back deformations with Fourier-transform profilometry", *Applied Optics*, 44(12), pp. 2266–2273, 2005.  
<https://doi.org/10.1364/AO.44.002266>
- [24] Genovese, K., Pappalettere, C. "Whole 3D shape reconstruction of vascular segments under pressure via fringe projection techniques", *Optics and Lasers in Engineering*, 44(12), pp. 1311–1323, 2006.  
<https://doi.org/10.1016/j.optlaseng.2005.12.005>
- [25] Arevalillo-Herráez, M., Cobos, M., García-Pineda, M. "A robust wrap reduction algorithm for fringe projection profilometry and applications in magnetic resonance imaging", *IEEE Transactions on Image Processing*, 26(3), pp. 1452–1465, 2017.  
<https://doi.org/10.1109/TIP.2017.2651378>
- [26] Su, X., Zhou, W. "Complex object profilometry and its application for dentistry", In: *Clinical Applications of Modern Imaging Technology II*, Los Angeles, CA, USA, 1994, pp. 484–489.  
<https://doi.org/10.1117/12.176592>
- [27] Yilmaz, S. T., Özüğürel, U. D., Bulut, K., Inci, M. N. "Vibration amplitude analysis with a single frame using a structured light pattern of a four-core optical fibre", *Optics Communications*, 249(4–6), pp. 515–522, 2005.  
<https://doi.org/10.1016/j.optcom.2005.01.032>
- [28] Hain, T., Eckhardt, R., Kunzi-Rapp, K., Schmitz, B. "Indications for optical shape measurements in orthopaedics and dermatology", *Medical Laser Application*, 17(1), pp. 55–58, 2002.  
<https://doi.org/10.1078/1615-1615-00047>
- [29] Huang, P. S., Jin, F., Chiang, F.-P. "Quantitative evaluation of corrosion by a digital fringe projection technique", *Optics and Lasers in Engineering*, 31(5), pp. 371–380, 1999.  
[https://doi.org/10.1016/S0143-8166\(99\)00019-6](https://doi.org/10.1016/S0143-8166(99)00019-6)
- [30] Chen, L. C., Chang, Y. W. "High accuracy confocal full-field 3-D surface profilometry for micro lenses using a digital fringe projection strategy", *Key Engineering Materials*, 364–366, pp. 113–116, 2008.  
<https://doi.org/10.4028/www.scientific.net/KEM.364-366.113>
- [31] Zuo, C., Huang, L., Zhang, M., Chen, Q., Asundi, A. "Temporal phase unwrapping algorithms for fringe projection profilometry: A comparative review", *Optics and Lasers in Engineering*, 85, pp. 84–103, 2016.  
<https://doi.org/10.1016/j.optlaseng.2016.04.022>
- [32] Su, X., Chen, W. "Fourier transform profilometry: A review", *Optics and Lasers in Engineering*, 35(5), pp. 263–284, 2001.  
[https://doi.org/10.1016/S0143-8166\(01\)00023-9](https://doi.org/10.1016/S0143-8166(01)00023-9)
- [33] Zhang, Z., Zhong, J. "Applicability analysis of wavelet-transform profilometry", *Optics Express*, 21(16), pp. 18777–18796, 2013.  
<https://doi.org/10.1364/OE.21.018777>
- [34] Huang, L., Kemao, Q., Pan, B., Asundi, A. K. "Comparison of Fourier transform, windowed Fourier transform, and wavelet transform methods for phase extraction from a single fringe pattern in fringe projection profilometry", *Optics and Lasers in Engineering*, 48(2), pp. 141–148, 2010.  
<https://doi.org/10.1016/j.optlaseng.2009.04.003>
- [35] Hansen, E. W. "Fourier transforms: principles and applications", John Wiley & Sons, 2014. ISBN 9781118479148 [online] Available at: [https://books.google.ro/books?hl=hu&lr=&id=YPauBAAQBAJ&oi=fnd&pg=PR11&dq=Hansen,+E.+W.+%22Fourier+transforms:+principles+and+applications%22,+John+Wiley+Sons,+2014.+ISBN+9781118901793+&ots=EQS9\\_LHQpe&sig=ggjNGXWp3ASUAjzr8Tag1qo3lyw&redir\\_esc=y#v=onepage&q=Hansen%2C%20E.%20W.%20%22Fourier%20transforms%3A%20principles%20and%20applications%22%2C%20John%20Wiley%20%26%20Sons%2C%202014.%20ISBN%209781118901793&f=false](https://books.google.ro/books?hl=hu&lr=&id=YPauBAAQBAJ&oi=fnd&pg=PR11&dq=Hansen,+E.+W.+%22Fourier+transforms:+principles+and+applications%22,+John+Wiley+Sons,+2014.+ISBN+9781118901793+&ots=EQS9_LHQpe&sig=ggjNGXWp3ASUAjzr8Tag1qo3lyw&redir_esc=y#v=onepage&q=Hansen%2C%20E.%20W.%20%22Fourier%20transforms%3A%20principles%20and%20applications%22%2C%20John%20Wiley%20%26%20Sons%2C%202014.%20ISBN%209781118901793&f=false) [Accessed: 28 February 2025]
- [36] Takeda, M., Ina, H., Kobayashi, S. "Fourier-transform method of fringe-pattern analysis for computer-based topography and interferometry", *Journal of the Optical Society of America*, 72(1), pp. 156–160, 1982.  
<https://doi.org/10.1364/JOSA.72.000156>
- [37] Badr, E. "Images in space and time: real big data in healthcare", *ACM Computing Surveys (CSUR)*, 54(6), 113, 2022.  
<https://doi.org/10.1145/3453657>
- [38] Zhang, D. "Wavelet transform", In: *Fundamentals of Image Data Mining: Analysis, Features, Classification and Retrieval*, Springer, 2019, pp. 35–44. ISBN 9783030179885  
[https://doi.org/10.1007/978-3-030-17989-2\\_3](https://doi.org/10.1007/978-3-030-17989-2_3)
- [39] MathWorks "MATLAB, (R2023a)", [computer program] Available at: <https://www.mathworks.com/help/releases/R2023a/matlab/> [Accessed: 15 May 2025]

- [40] Mandlburger, G. "A review of active and passive optical methods in hydrography", *The International Hydrographic Review*, 28, pp. 8–52, 2022.  
<https://doi.org/10.58440/ihr-28-a15>
- [41] MathWorks "Wavelet Toolbox", [online] Available at: <https://www.mathworks.com/help/wavelet/> [Accessed: 28 February 2025]
- [42] Abdulmunem, M. E., Badr, A. A. "Hilbert Transform and its Applications: A survey", [pdf] *International Journal of Scientific and Engineering Research*, 8(2), pp. 699–704, 2017. Available at: [https://www.researchgate.net/profile/Ameer-A-Badr/publication/337935057\\_Hilbert\\_Transform\\_and\\_its\\_Applications\\_A\\_survey/links/5df5283fa6fdcc2837225766/Hilbert-Transform-and-its-Applications-A-survey.pdf](https://www.researchgate.net/profile/Ameer-A-Badr/publication/337935057_Hilbert_Transform_and_its_Applications_A_survey/links/5df5283fa6fdcc2837225766/Hilbert-Transform-and-its-Applications-A-survey.pdf) [Accessed: 28 February 2025]
- [43] Singh, A. "Survey paper on Hilbert transform with its applications in signal processing", [pdf] *International Journal of Computer Science and Information Technology*, 5(3), pp. 3880–3882, 2014. Available at: <https://citeseerx.ist.psu.edu/document?repid=rep1&type=pdf&doi=29531bb4effcd823f55b0c0e6ec58b0e398f7c6e> [Accessed: 28 February 2025]
- [44] Meng, X., Wang, F., Liu, J., Chen, M., Wang, Y. "Phase shifting profilometry based on Hilbert transform: An efficient phase unwrapping algorithm", *Journal of Applied Physics*, 131(19), 193104, 2022.  
<https://doi.org/10.1063/5.0084695>
- [45] Ayenu-Prah, A. Y., Attoh-Okine, N. O. "Comparative study of Hilbert–Huang transform, Fourier transform and wavelet transform in pavement profile analysis", *Vehicle System Dynamics*, 47(4), pp. 437–456, 2009.  
<https://doi.org/10.1080/00423110802167466>
- [46] Chatterjee, A., Singh, P., Bhatia, V., Prakash, S. "Hilbert transform based phase extraction algorithm for fringe projection profilometry", In: *2018 3rd International Conference on Microwave and Photonics (ICMAP)*, Dhanbad, India, 2018, pp. 1–2. ISBN 9781538609347  
<https://doi.org/10.1109/ICMAP.2018.8354561>